

MONITORING DIURNAL UNDERWATER TEMPERATURE USING FY-2C IN POYANG LAKE NATURE RESERVE, CHINA

Xiao Zhou^{1,2} Valentijn Venus² Zhang Haitao¹

¹ Beijing Institute of Surveying and Mapping Beijing P.R.China 100038

² International Institute For Geo-Information Science And Earth Observation
Enschede The Netherlands

Commission VIII, WG VIII/7

KEY WORDS: Satellite Remote Sensing, Hydrographic Features, Environmental Monitoring, FY-2C, Underwater Water Temperature, Submerged Aquatic Vegetation Simulation Mode, Poyang Lake Nature Reserve

ABSTRACT:

Significant numbers of bird species forage on the tubers of the submerged aquatic species. This resource is difficult to map due to the submerged nature of these species. Because the temperature is the primary driving factor of photosynthesis in these vegetation species, it is possible to map the distribution and biomass production of these submerged species indirectly. For the relative short growth date of the submerged aquatic species, geostationary satellites are of particular interest because they depict the diurnal cycle. So far, however, few researches related high temporal resolution satellite data to monitor underwater temperature. In this paper we explored the possibility of using *Fengyun-2C* meteorological satellite imagery as the primary data source to monitor the diurnal underwater temperature. We firstly retrieved lake surface temperature and radiation using FY-2C imagery and validated it by ground observed data. Secondly, the relationship between the environmental factors and underwater temperature is analyzed. Then two regression models were built respectively for day-time and night-time for the variance of the underwater temperature. We modeled day-time underwater temperature by water depth, turbidity, water skin solar radiation and temperature. Water surface temperature and water depth were used for night-time model. Finally, we attempted to apply these models to predict the temperature to see how far this method can go. The result showed that this method explained 72 % of the variance of the diurnal underwater temperature. The standard error of the prediction was 0.5°C. So this method is capable of predicting the spatial distribution of underwater temperature.

1. INTRODUCTION

Many bird species feed on submerged aquatic vegetation in shallow lakes. The attractiveness of migratory stopover or overwintering grounds to these bird species largely depends on the total standing tuber biomass that forms the main component of their diet (Taylor 2005). As mapping the total standing biomass of aquatic vegetation from remotely sensed imagery remains challenging due to the submerged nature of these species, other techniques deserve more attention. Some studies and field observation indicate that temperature is the primary driving factor of photosynthesis in these vegetation species (Best 2001; Gulati and Donk 2002), argued to be even more important than light absorption (Ort 2001; Cumba 2006). As the strong relationship exists, it is possible to map the distribution and biomass production of these submerged species indirectly.

The retrieval of underwater temperature variations from satellites observations has seldom been explored, though water surface temperature has been studying widely in many researches (Bussieres et al. 2002; Becker and Daw 2005). In the past, mathematical modeling of underwater temperature based on field surveys had received considerable attention (Hostetler and Bartlein 1990). Generally, however, these mathematical models are too complicated and have strict physical parameters for predicating the temperature in deep waters, such as reservoir; on the other hand, most inputs to the model have not been obtained by remote sensing techniques. In this case, it is possible and necessary for us to rebuild a model for estimating of underwater temperature which is suitable to the shallow lake using solar radiation, water clarity and lake surface temperature.

Remote sensing offers the possibility to measure solar radiation, surface water temperature and water clarity. For example, Bisht et al. (2005) estimated radiation changes for clear sky days from moderate resolution imaging spectroradiometer (MODIS) observations; while Handcock et al. (2006) studied the accuracy and uncertainty of water temperature estimates from the thermal-infrared band of ASTER, MODIS and Landsat ETM+ images; and Nellis and Wu (1998) employed TM to estimate the spatial and temporal variations of water clarity.

Nowadays, it has successfully been able to use imagery from polar-orbiting satellites to estimate solar radiation and water temperatures. However, due to their relative low temporal resolution too few clear sky observations remain to satisfy our temporal model requirements. In other words, surface temperature and radiation have a strong diurnal cycle, which cannot be captured at the temporal resolution (approximately one or two times per day; effectively maybe every 10-15 days depending on cloud cover) of the polar orbiters. The inaccuracies in daily gross assimilation estimates caused by this phenomenon can accumulate to the unacceptable level rendering the model results useless. So a formidable challenge lies in the use of the high temporal resolution satellite data to provide estimates of water temperature and insolation commensurate with the temporal requirement of our objective.

Feng-Yun-2C meteorological satellite (FY-2C), a relatively new geo-stationary meteorological satellite operated by the General National Satellite Meteorological Centre (NSMC) of China observes a large part of Asia centered at 105 degrees east every hour (NSMC 2005). The spatial resolution is 1.25 km for the

visible channel and about 5 km for the infrared and water vapour channels. As we know, the variety of solar radiation and surface temperature is very little in the area of 1 to 25 km². So the resolutions of FY-2C satisfy the requirement of study. These characteristics make *Feng-Yun-2* data a good data source for estimating surface radiation and temperature in high temporal resolution.

The objective of this paper is to monitor the underwater temperature for aquatic vegetation. Based on estimating water (skin) temperature and solar irradiance using satellite data from FY-2C imagery, we built the day-time and night-time model separately to simulate the underwater temperature with surface radiation, surface temperature and water clarity using multiple linear regression techniques.

2. STUDY AREA

Poyang Lake National Nature Reserve in Jiangxi Province is at the southern bank of the middle and lower reaches of the Yangtze River. The reserve was established in 1988 to conserve the endangered Siberian crane which overwinters almost uniquely in this area. The water level fluctuates seasonally from low in winter to high in July and August.

3. METHODS AND RESULTS

3.1 Radiation

Radiation was estimated for every hour interval from the FY-2C visible channel data acquired in the period 2006-07-08 to 2006-08-04. The number of day-time was 28. The estimations were validated using ground observed data for clear sky-conditions and overcast conditions separately.

Compared with the traditional empirical approach to estimate cloud index, the Heliosat method(Dagestad and Olseth 2005) was used to derive surface solar radiation in cloud free and cloudy situations in the study area. This method deals with atmospheric and cloudy extinction separately. The results showed that the Heliosat method provides satisfactory accuracy for the estimation of radiation. The accuracy of the method and the results were validated using ground radiation data. A good agreement was found in one month analysis. The RMSE values varied from 14.4 Wm⁻² to 89.5 Wm⁻². For these RMSE values, the R² ranged from 0.75 to 0.99. The highest R² corresponded to the lowest RMSE. The average R² is 0.913 Wm⁻² and average RMSE is 57.2 Wm⁻².

3.2 Lake surface Temperature

We used a derivation of the general split-window algorithms enhanced for satellite viewing angle-effects to estimate land surface temperature (Sun and Pinker 2003). This method takes advantage of the differential absorption in spectral windows, centered at 10.8 μm and 12 μm for the geostationary satellite, to correct for atmospheric effects and describes the surface temperature in terms of a simple linear combination of brightness temperatures as measured in both thermal channels. This algorithm is given below:

$$T_s(i) = a_0(i) + a_1(i)T_{11} + a_2(i)(T_{11} - T_{12}) + a_3(i)(T_{11} - T_{12})^2 + a_4(i)(\sec \theta - 1)$$

Where T_s is the surface temperature measurement, T_{11} and T_{12} are the brightness temperatures at 10.8 μm and 12 μm channels of FY-2C, respectively, θ is the satellite zenith angle and a_0 to a_4 are coefficients that have been determined to minimize the error using the Moderate Resolution Atmospheric Radiance and Transmittance Model (MODTRAN) (Sun and Pinker 2003). i is the index of surface types which is obtained from 1km resolution global land cover map from The Department of Geography at the University of Maryland. This product includes 14 International Geosphere-Biosphere Programme (IGBP) classes (Defries *et al.* 2000)

Land surface temperature, however, is retrieved from thermal channels of FY-2C data only in clear-sky conditions when LST is not mixed with cloud-top temperature. The Thermal Infrared signals (TIR) can't penetrate thick clouds. It is difficult to correct the effect of thin clouds on the TIR signals without knowing the exact optical depth of thin clouds (Sun *et al.* 2006). So all clouded pixels were excluded from the calculations.

The validation of the results showed the range of R² is from 0.79 to 0.87 and RMSE is from 0.3 K to 2.5 K.

3.3 Night-time underwater temperature model

We used underwater temperature logging data to obtain the quantitative relationship. So the square of the coefficients of determination (R²) between diurnal cycle underwater temperature and surface temperature were computed to determine the relationship. The result is illustrated in 2D-correlation plots (Figure 1). Each box represents the R² value between surface temperature and under water temperature at each depth.

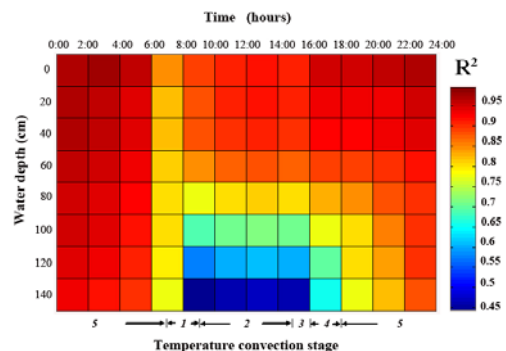


Figure 1 2D-correlation plots that show the square of the correlation coefficient (R²) between surface temperature and under water temperature at each depth

In Figure 1, the relationship from 18:00 to next day 6:00 was better than other time. The correlation coefficient are not satisfactory during day-time due to it also links to some other natural factors. Further analysis showed that the underwelling temperatures are very close to the surface temperature between sunset and sunrise period. Figure 2 below shows the distribution of surface and underwater temperatures. As can be seen from the figure, there is not a great deal of difference between underwelling temperature and surface temperature in this stage. The difference peaked at 18:00 and the biggest difference appeared between the surface temperature and temperature at

140cm with the value 0.41 °C. The difference remained steady from 20:00 to 6:00, only between 0.01 – 0.21 °C.

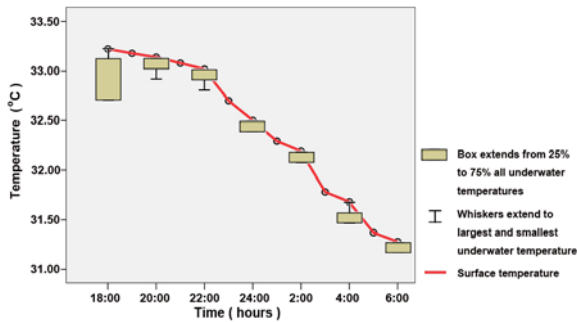


Figure 2 Box plot showing the distribution of surface and underwater temperatures

In combination with the daily range of surface water temperature is about 4-10 °C and 2-4.5 °C at the bottom of the lake (Wu and Ji 2002), 0.4 °C is so tiny that we can ignore this point. So we can safely assume the vertical temperatures in the lake have the same value with the surface temperature during this period of the day.

3.4 Day-time underwater temperature model

For day-time, we did regression analysis with dependent variables. First, we find a strong linear relationship ($R^2 = 0.9896$) which examines the relationship between temperature and water depth, in the same water clarity ($SSC = 238 \text{ mg/L}$) and same surface radiation (950 Watt/m^2). Second, we put some temperature loggers under the water at the same depth (50cm) at same water clarity (same $SSC = 238 \text{ mg/L}$). By a Quadratic Fit, the R^2 can reach 0.95. Third, we find the relationship between water temperature at 50 cm depth and surface temperature with the same water clarity (same $SSC = 238 \text{ mg/L}$) and same surface radiation (950 Watt/m^2). Strong linear relationship ($R^2 = 0.935$) is observed. Now combine these three relationships, we are able to calculate the underwater temperature by and given surface radiation, surface temperature and water depth. We get the result below:

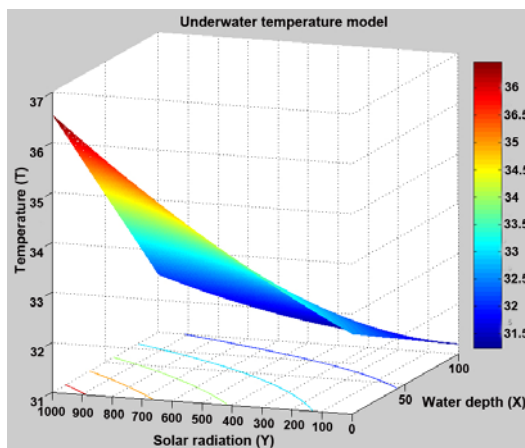


Figure 3 Underwater temperature model

In the figure above, X axis is the water depth, with the unit of centimetre; Y axis is the radiation at surface of lake, with the unit of Watt/m^2 , T axis is the underwater temperature, and the unit for temperature is degree centigrade.

We can see from this graph, the underwater temperature is high, when the water depth is low and surface radiation is high, which means in the shallow water and shining day, the vegetation at the bottom of lake can receive more temperature. And the peak of the 3-D curve converge with temperature axis at 36.5 °C where is value of the surface temperature.

Then, we considered SSC in our model. Considering the physical characteristics of the model, water clarity just works when water depth changing. If estimating the temperature just under the water level (water depth = 0), the water clarity doesn't contribute for the temperature. So the water depth deeper, the more water clarity influences. In this case, we multiply new variable (link to SSC) with water depth.

After doing the linear stepwise regression using field data, we get the final model ($R^2=0.923, \text{RMSE}=0.51 \text{ °C}$). By this model, we can calculate the underwater temperature at any depth and water clarity with any radiation and temperature at surface of lake.

3.5 Application of day-time and night-time models

In order to see how far this method can go, we attempted to apply it to predict the temperature at the bottom of the lake, where aquatic vegetation grows, according to water clarity retrieved from MODIS, solar radiation and lake surface temperature from FY-2C and water depth. We hope could generate underwater temperature maps with sufficient accuracy.

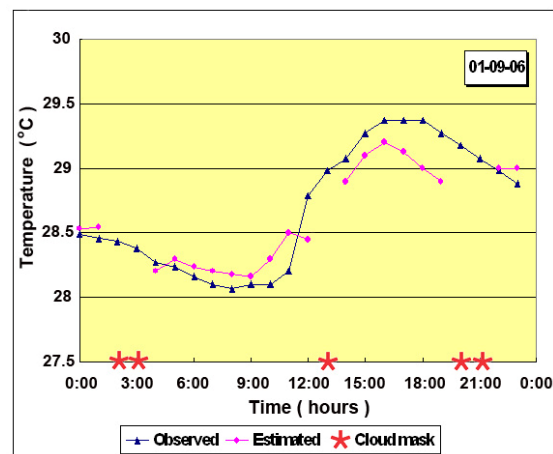


Figure 4 shows the comparison between estimated and observed diurnal temperature at the bottom of lake on 1st Sep. 2006.

Figure 4 above shows the comparison between estimated and observed diurnal temperature on 1st Sep. 2006. Due to the influence of cloud mask on LST estimation, the estimated temperatures were not available between 12:00 - 14:00, 19:00 - 22:00 and 1:00 – 4:00 hours.

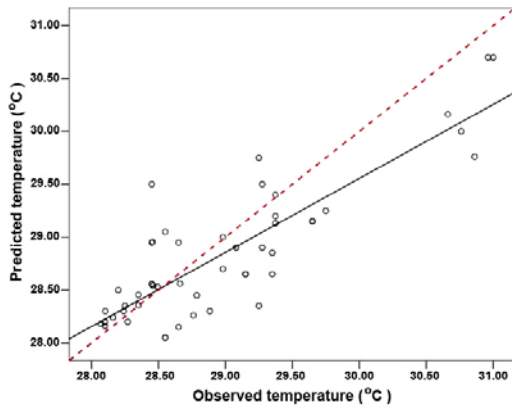


Figure 5 Scatter of observed versus predicted temperature at the bottom of lake on 1st Sep. 2006

The Figure 5 shows the fitted regression line against the expected line for an unbiased predictor. The dotted line corresponds to an unbiased predictor, while the solid line represents the observed linear regression relationship. The Standard error of estimation (RMSE) is 0.5 °C with $R^2 = 0.72$.

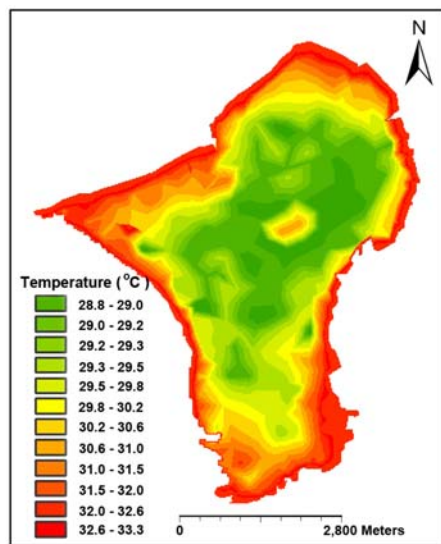


Figure 6 Underwater temperature map at the bottom of the Dahuchi Lake at 14:00 01-09-06

Figure 6 illustrates that the distribution map of underwater temperature at the bottom of the lake at 14:00 1st Sep. 2006.

4. DISCUSSION

In the night-time model, we did regression between surface temperature and underwater temperature at various water depths. The results in the test lake were better during the evening than the day, presumably due to the greater influence of radiation and latent heat fluxes during daylight hours.

According to the regression analysis in the day-time model, there is a significant relationship between surface radiation, surface temperature, water depth and SSC. Considered about the light attenuation in the water, water clarity is an important environmental indicator for detecting the underwater temperature. But after importing the SSC as the input of the

model, the accuracy was decreased from 0.98 to 0.92. The main reason for that is the SSC span we obtained from the field was relatively narrow. It was just from 140 to 300 mg/L. The narrow SSC span, it makes the influence of SSC not represented adequately (Nellis and Wu 1998).

In this study we showed that the model we built for both day and night explained 72 % of the variance of the natural logarithm of underwater temperature with the RMSE of 0.5 °C.

5. CONCLUSION

This paper emphasizes the importance of underwater temperature, while applying remote sensing techniques. This could significantly reduce the uncertainties and the degree of "erroneous prediction". Map displaying underwater temperature sites where it is suit for vegetation growth could be used to significantly reduce the influence of man-made and ecological destruction. These will support efficient habitat ranking to protect ecosystems and predict the future habitat sites of wild birds.

REFERENCES

- Taylor, J. P. a. L. M. S. (2005). "Migratory bird use of belowground foods in moist-soil managed wetlands in the Middle Rio Grande Valley, New Mexico." *Wildlife Society Bulletin* 33(2): 574-582
- Best, E. P. H. and W. A. Boyd (2001). A Simulation Model for Growth of the Submersed Aquatic Macrophyte American Wildcelery (*Vallisneria americana* Michx.): P.108.
- Gulati, R. D. and E. v. Donk (2002). "Lakes in the Netherlands, their origin, eutrophication and restoration: state-of-the-art review." *Hydrobiologia* 478(1-3): 73-106.
- Ort, D. R. (2001). "When there is too much light." *Plant Physiol.* 125(1): 29-32.
- Bussieres, N., D. Versegny and J. I. MacPherson (2002). "The evolution of AVHRR-derived water temperatures over boreal lakes." *Remote Sensing of Environment* 80(3): P.373-384.
- Becker, M. W. and A. Daw (2005). "Influence of lake morphology and clarity on water surface temperature as measured by EOS ASTER." *Remote Sensing of Environment* 99: 288-294.
- Hostetler, S. W. and P. J. Bartlein (1990). "Simulation of lake evaporation with application to modeling lake level variations of Harney-Malheur lake, Oregon. ." *Water Resour* 26: 2603-2612.
- Bisht, G., V. Venturini, S. Islam and L. Jiang (2005). "Estimation of the net radiation using MODIS (Moderate Resolution Imaging Spectroradiometer) data for clear sky days." *Remote Sensing of Environment* 97: 52-67.
- Handcock, R. N., A. R. Gillespie, K. A. Cherkauer, J. E. Kay, S. J. Burges and S. K. Kampf (2006). "Accuracy and uncertainty of thermal-infrared remote sensing of stream temperatures at multiple spatial scales." *Remote Sensing of Environment* 100(4): 427-440.

Nellis, M. D. and J. Wu (1998). "Remote sensing of temporal and spatial variations in pool size, suspended sediment, turbidity, and Secchi depth in Tuttle Creek Reservoir." Geomorphology **21**: 281-293.

NSMC (2005). FY-2C Product User Instruction.

Dagestad, K. F. and J. A. Olseth (2005). "An alternative algorithm for calculating the cloud index." University of Bergen.

Sun, D. and R. T. Pinker (2003). "Estimation of land surface temperature from a Geostationary Operational Environmental

Satellite (GOES-8)." JOURNAL OF GEOPHYSICAL RESEARCH **VOL.108**(No. D11): 4326

Defries, R. S., M. C. Hansen, J. R. G. Townshend, A. C. Janetos and T. R. Lovelands (2000). "A new global 1-km dataset of percentage tree cover derived from remote sensing." Global Change Biology **6(2)**: 247-254

Sun, D., M. Kafatos, R. T. Pinker and D. R. Easterling (2006). "Seasonal Variations in Diurnal Temperature Range From Satellites and Surface Observations." IEEE TRANSACTIONS ON GEOSCIENCE AND REMOTE SENSING **Vol.44**(No.10).

